International Journal of Thermophysics, Vol. 20, No. 2, 1999

Simultaneous Measurement of Specific Heat Capacity, Thermal Conductivity, and Thermal Diffusivity by Thermal Radiation Calorimetry

K. Hisano,[1,2] S. Sawai,[1] and K. Morimoto[1]

Thermal radiation calorimetry has been applied to measure the thermal diffusivity of a solid specimen, along with simultaneous measurements of specific heat capacity and thermal conductivity. In this calorimeter, a disk-shaped solid specimen whose surfaces are blackened is heated and cooled slowly on one face by irradiation in a vacuum chamber. A quasi-steady-state approximation in which a linear temperature gradient within the specimen was assumed is considered in the analysis. The validity of this approximation was confirmed by the results of computer simulation based on the control-volume method. Measurements of Pyroceram 9606 and Pyrex 7740 by use of thermocouples in the temperature range between 250 and 400°C gave values consistent with those obtained by previous authors, within experimental error, for all three thermophysical properties.

KEY WORDS: calorimetry; diffusivity; emissivity, heat capacity; radiant exchange; simultaneous measurement; thermal conductivity.

1. INTRODUCTION

Simultaneous measurements of thermal diffusivity, thermal conductivity, and specific heat capacity have been performed for a solid specimen by Peralta *et al.* [1] by means of impulse-response photopyroelectric spectrometry in the temperature range just below room temperature. The impulse response technique used in this measurement requires neither calibration nor preliminary normalization to provide simultaneous measurements, unlike conventional photothermal techniques. Recently, a conventional method based on thermal radiation calorimetry (TRAC) has allowed

[1] Department of Mathematics and Physics, National Defense Academy, Hashirimizu 1-10-20, Yokosuka 239-8686, Japan.

[2] To whom correspondence should be addressed.

0195-928X/99/0300-0733$16.00/0

simultaneous measurements of specific heat capacity and thermal conductivity for an insulating disk-shaped specimen in a temperature range just above 450°C [2]. If we know the values of two of the three quantities, it is possible to obtain the other since they are not independent. However, if it is possible to measure all three physical quantities experimentally and also simultaneously, a *self-check* of the reliability of the obtained values can be performed. For example, we may check the reliability and self-consistency of the values obtained for an unknown specimen by comparing the specific heat capacity obtained experimentally with that calculated from the thermal conductivity and the thermal diffusivity.

Although the theoretical description has been presented previously [3], until now it has not been possible to use the TRAC to measure thermal diffusivity because a noncontact temperature measurement of the specimen surfaces was not sufficiently accurate to obtain a reliable value. In the present experiment, thermocouples attached directly to the specimen have been used to obtain the thermal diffusivity as well as the other two quantities simultaneously for Pyroceram 9606 and Pyrex glass 7740 in the temperature range from 250 to 400°C. Note that for a Pyroceram specimen, thermal conductivity measurements have not previously been successful in the range below 400°C. These are useful reference materials because the thermophysical properties are relatively well known at elevated temperatures and also because the coefficient of the temperature dependence of the thermal conductivity is of opposite signs in the two materials [4].

2. EXPERIMENT

A theory of the present calorimeter has already been presented in detail in previous papers [2, 3]. As shown in the schematic in Fig. 1, we consider a one-dimensional system in which a disk-shaped specimen of thickness L in a vacuum chamber is heated and cooled on one face by irradiation, producing a small change in the time rate of the specimen temperature. The quasi-steady-state approximation gives the following relations at the same back surface temperature ($T_0 = T'_0$) facing the chamber wall, when the temperature change rate is the same for both heating and cooling modes:

$$\lambda = \frac{2L}{T_L + T'_L - 2T_0} \varepsilon I_0 \tag{1}$$

$$a = \frac{\lambda}{C_p \rho} = \frac{L^2}{2(T_L - T'_L)} \left\{ \left(\frac{\partial T}{\partial t} \right)_{\text{av}} - \left(\frac{\partial T}{\partial t} \right)'_{\text{av}} \right\} \tag{2}$$

where λ, a, C_p and ρ are the thermal conductivity, the thermal diffusivity, the specific heat capacity, and the density, respectively. T_L is the front surface temperature facing the heater. The radiant power per unit area (power density) emitted by the specimen to the room temperature chamber wall for a perfect absorber I is given as $I=\sigma(T^4-T_r^4)$, where σ and T_r are the Stefan–Boltzmann constant and room temperature, respectively. The prime refers to the cooling mode. Similarly, the following relation is derived for the specific heat capacity at the same temperature of the front surface ($T_L=T'_L$). Because of small changes of C_p and ρ with temperature for a regular material, C_p shows no abrupt change in the temperature dependence:

$$C_p=\frac{E_h(I_h-I'_h)-\varepsilon(I_0-I'_0)}{\rho L\{(\partial T/\partial t)_{\mathrm{av}}-(\partial T/\partial t)'_{\mathrm{av}}\}} \tag{3}$$

where E_h is the "effective" emissivity [2, 3]. I_0 and I'_0 are the radiant power densities emitted from the back specimen surface for heating and cooling modes, respectively. I_h and I_h' are the radiant power densities emitted from the heater for both modes. I_L and W_h in Fig. 1 are the radiant power density

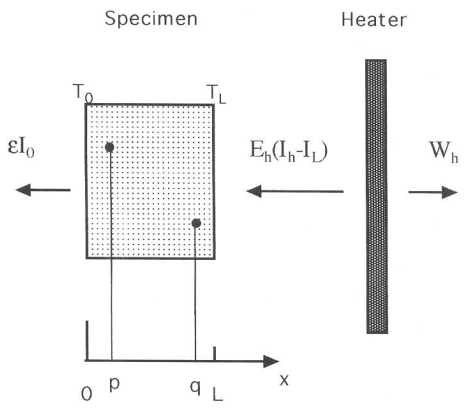

Fig. 1. Schematic for thermal radiation calorimetry. Thermocouples are attached at positions p and q in the x direction. I_0 and I'_0 are the radiant power densities emitted from the back specimen surface for heating and cooling modes, respectively. I_h and I'_h are the radiant power densities emitted from the heater for both modes. I_L and W_h are the radiant power density emitted from the front specimen surface and the output signal for the radiant power from the heater, respectively.

emitted from the front specimen surface and the output signal for the radiant power from the heater, respectively. Equations (1)–(3) imply that the three thermophysical quantities are obtained experimentally and simultaneously because the terms on the right-hand side of these equations are evaluated experimentally. However, the values obtained are those for the specimen with a slightly nonhomogeneous temperature.

Figure 2 shows the schematic configuration of the heater and the specimen, which are placed in a water-cooled vacuum chamber maintained to better than 10^{-3} Pa. The specimen (25 mm in diameter) is supported by two alumina tubes (1 mm in diameter) placed about 6 mm above the heater made from a graphite sheet (5 cm square and 0.5 mm thick). Unlike the previous case, the temperature gradient within the specimen was measured by the use of two alumel–chromel thermocouples attached directly to the specimen. The thermocouple sheathed in a tube of Inconel 600 (0.5-mm diameter) was set in a hole (0.75-mm diameter and 6-mm depth) drilled in the side. Because of the mismathch between the sheath diameter and the hole diameter, graphite adhesive was used to achieve good thermal contact between the specimen and the thermocouple. Pyrex glass (25 mm in diameter and 5 mm thick) and Pyroceram 9606 (25 mm in diameter and 4.7 mm thick) specimens were prepared. The entire surfaces of the specimens were coated with copper metal by vacuum evaporation

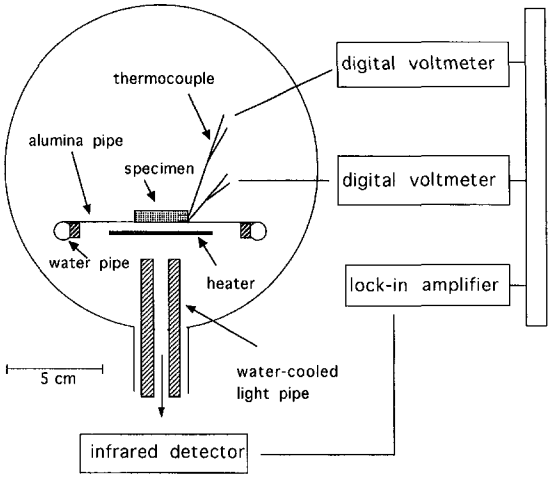

Fig. 2. Schematic diagram of heater part. A specimen supported on two thin alumina tubes is heated and cooled by a graphite flat heater. The temperature distribution within the specimen is measured with two thermocouples. The infrared radiant power from the heater is measured with a pyrometer.

before blackening the front and back surfaces. The surfaces of the heater and the specimens were blackened with colloidal graphite (Acheson, Electrodag 188). The thermocouple hole positions of p and q in the x direction are, respectively, 1.02 ± 0.01 mm and 3.98 ± 0.01 mm for the Pyrex specimen and 1.03 ± 0.01 and 4.01 ± 0.01 for the Pyroceram specimen. The thermocouple separation was about 13 mm measured at the side surface.

Using a pyrometer, the radiant power from the heater was measured instead of the heater temperature T_h. The heater current was controlled so that the ramp rate becomes about $5°C \cdot min^{-1}$ for both heating and cooling modes. Data for T_p, T_q, and W_h were collected every 15 s for both modes. The "effective" emissivity, E_h/G_h, obtained by use of copper metal (25 mm in diameter and 3 mm thick) was confirmed to be constant for the range from 200 to 400°C, where G_h is a gain factor for the electric circuit for the pyrometer. The emissivity of velvet-like graphite surfaces, ε, was assumed to be 0.93 ± 0.02 in the analysis because the emissivity obtained from the room temperature infrared spectrum is from 0.9 to 0.96 in the temperature range from 200 to 800°C and the "effective" emissivity for the configuration used in the previous paper is constant in the range from 250 to 400°C [5].

3. RESULTS AND DISCUSSION

In order to confirm the validity of the quasi-steady-state approximation described above, a computer simulation based on the control-volume method [7] was performed at 200°C for Pyroceram 9606. Values of parameters such as thermophysical quantities necessary for the calculation were taken from the literature [4, 8, 9]. The configuration of the heater and specimen and the emissivity were assumed to be the same as described previously [5]. Figure 3 shows the results of the calculation for a 5-mm thickness with a ramp rate of $5°C \cdot min^{-1}$ ignoring the heat loss through the specimen support. The solid line indicates the results at steady state. The spatial change rate within the specimen is almost linear for both modes in which case the temperature distribution within the specimen is almost parabolic. The heat loss through the support cannot be evaluated quantitatively in the present experiment. However, a similar calculation was performed assuming the heat loss to be proportional to $T_L - T_r$. The results indicate that the temperature distribution is nearly exactly the same as that obtained by ignoring the loss. The only difference is that the heater temperature required to achieve a back surface temperature of 200°C is not the same.

It is necessary to obtain the temperatures of both specimen surfaces from the temperatures at $x = p$ and q. The procedure to obtain both surface temperatures is as follows. First, we find the steady-state temperatures

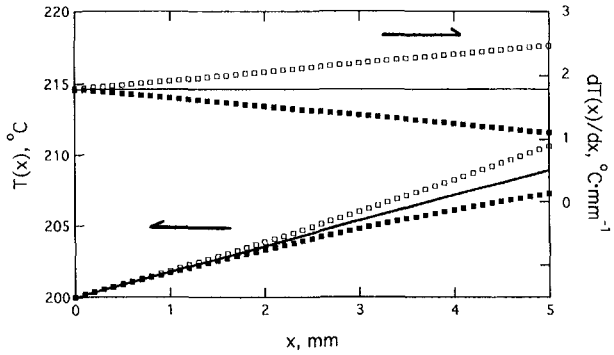

Fig. 3. Temperature distribution and gradient within the Pyres specimen obtained by computer simulation based on the control-volume method. The bad surface temperature, T_0, is fixed at 200°C and the temperature change rate is $2°C \cdot mm^{-1}$. (□) Heating; (■) cooling; (—) steady state.

at positions $x = p$ and q from T_p and T_q for the heating and cooling modes at various temperatures (see Fig. 3). A linear temperature distribution within the specimen for steady state is then obtained at various temperatures from the results. We are therefore able to obtain an analytical parabolic function for the distribution in the quasi-steady state. Figure 4 shows the temperature dependences of $T_q - T_p$ and $T_L - T_0$ estimated from T_q and T_p for the Pyroceram specimen in the range from 250 to 400°C. Compared with noncontact measurements [2, 3], the measurement using

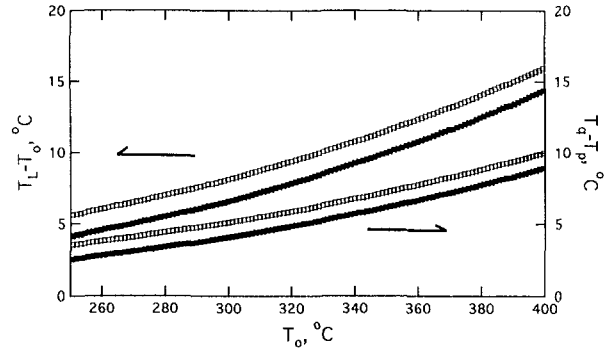

Fig. 4. Temperature differences of $T_L - T_0$ and $T_q - T_p$ for the Pyroceram specimen for heating and cooling modes at various back surface temperatures, T_0. T_L and T_0 were calculated from T_q and T_p. (□) Heating; (■) cooling.

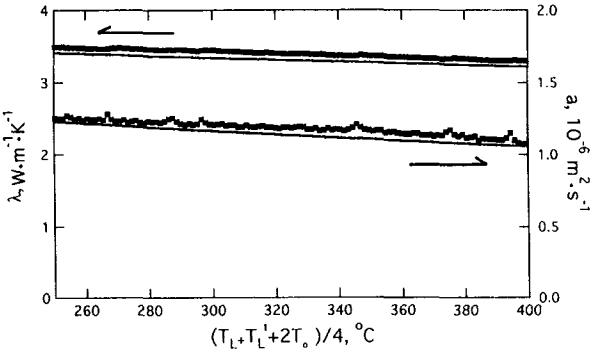

Fig. 5. The thermal conductivity and the thermal diffusivity of the Pyroceram specimen obtained experimentally from Eqs. (1) and (2). The thin solid line for the thermal conductivity shows the temperature dependence estimated from a least-squares fit using the experimental values obtained by previous authors [4, 9], while that for the thermal diffusivity is the temperature dependence obtained by Suliyanti et al. [10].

two thermocouples gives a much better result on the temperature difference between the surfaces. Figures 5 and 6 show the thermal conductivity, the diffusivity, and the specific heat capacity obtained simultaneously from Eqs. (1)–(3). The thin solid lines for the thermal conductivity and the specific heat capacity in these figures are the results of a least-squares fit

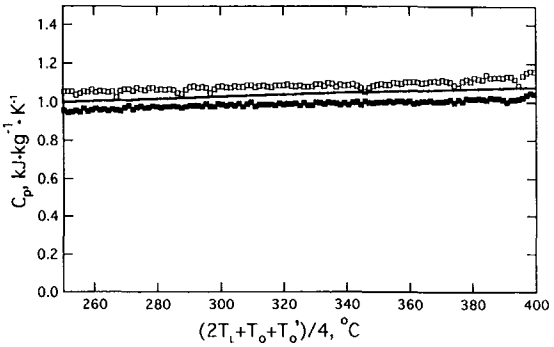

Fig. 6. The specific heat capacity of the Pyroceram specimen. The filled squares indicate the experimental values obtained from Eq. (3). The open squares indicate the values calculated from the thermal conductivity and thermal diffusivity shown in Fig. 5. The thin solid line shows the temperature dependence estimated from a least-squares fit using the experimental values obtained by previous authors [8].

using the values obtained by previous authors [4, 8, 9], while the line for the thermal diffusivity is the result of a least-squares fit performed by Suliyanti *et al.* [10] using the experimental values obtained by means of the laser flash method. The filled squares in Fig. 6 are the specific heat capacities obtained experimentally from Eq. (3), in which E_h and I_h are replaced by E_h/G_h and W_h, respectively. The open squares are the specific heat capacities calculated from the thermal conductivity and the thermal diffusivity shown in Fig. 5 with a density of 2601 $kg \cdot m^{-3}$ [8]. The results for the Pyrex specimen are similarly shown in Figs. 7 and 8. The filled squares in Fig. 8 are the specific heat capacity obtained experimentally from Eq. (3), while the open squares are those calculated from the thermal conductivity and the thermal diffusivity shown in Fig. 7 with a density of 2226 $kg \cdot m^{-3}$ [8]. The thin solid lines in these figures are the results of a least-squares fit using the values obtained by previous authors [4, 8, 9].

The largest source of error in the present measurement is caused by a tolerance of ± 0.15 mm in the distance between positions p and position q in the x direction. This tolerance is caused by the difference between the thermocouple diameter and the diameter of the holes drilled in the side. The errors caused by this tolerance are about $\pm 10\%$ for the thermal diffusivity and for the thermal conductivity. The total relative errors calculated from Eqs. (1)–(3) are therefore about ± 20, ± 15, and $\pm 10\%$ for the thermal diffusivity, the thermal conductivity, and the specific heat capacity, respectively. As far as the thermal conductivity and the specific heat capacity are concerned, the error is larger than that involved in previous noncontact measurements [2] in which the major source of the

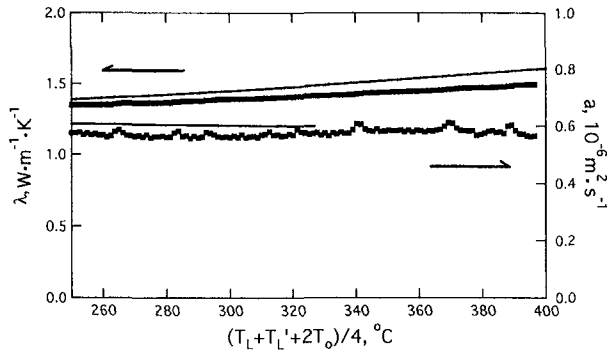

Fig. 7. The thermal conductivity and thermal diffusivity of the Pyres glass specimen obtained experimentally from Eqs. (1) and (2). The thin solid lines show the temperature dependences estimated from a least-squares fit using the experimental values obtained by previous authors [4, 9].

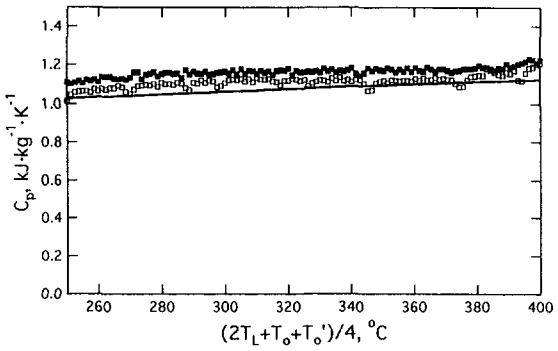

Fig. 8. The specific heat capacity of the Pyrex glass specimen. The filled squares indicate the experimental values obtained from Eq. (3). The open squares indicate the values calculated from the thermal conductivity and the thermal diffusivity shown in Fig. 7. The thin solid line shows the temperature dependence estimated from a least-squares fit using the experimental values obtained by previous authors [8].

error was caused by the temperature measurement of the specimen surfaces. If the errors caused by the tolerance are ignored, the relative errors become ± 10, ± 5, and $\pm 5\%$, respectively. We may reduce the errors in measurements with a thicker specimen by use of a guard reflector for the side surface to reduce radiation loss as much as possible. In the present experiment, no significant difference has been observed in the results obtained by use of a guard reflector. This is presumably because of the copper coat on the side surface. The present method has so far given larger errors compared with sophisticated photothermal techniques such as the photopyroelectric spectromer [1] and the laser-flash calorimeter [10]. As far as the present authors are aware, the photothermal methods give an uncertainty to within 5%. Despite this disadvantage, the TRAC gives the following advantages. The temperature dependence of thermophysical parameters is obtained in a relatively short time and at low cost. It takes only about 2 h to cover a temperature range of 200°C after reaching a good vacuum. Continuous (as opposed to discrete) temperature data can be obtained. In addition, the calorimeter with two thermocouples enables us to obtain the thermal diffusivity. Therefore, all three thermophysical parameters are obtained experimentally and simultaneously from Eqs. (1)–(3), unlike the case of a noncontact measurement. As shown in Figs. 6 and 8, the self-check of reliability of three parameters is performed by confirming that the values of specific heat derived experimentally from Eq. (3) are consistent with those calculated from the thermal conductivity and thermal diffusivity within our experimental accuracy.

4. CONCLUSION

Radiation calorimetry has been applied to simultaneous measurements of the specific heat capacity, the thermal conductivity, and the thermal diffusivity of thermal insulators. In this calorimeter, a disk-shaped solid specimen whose surfaces are blackened is heated and cooled slowly on one face by irradiation in a vacuum chamber. The temperature difference between the faces was obtained from the temperatures at two positions within the specimen measured with thermocouples, which made it possible to measure the thermal diffusivity. A quasi-steady-state approximation, in which a linear temperature gradient within the specimen was assumed, was applied in the analysis. This was confirmed to be acceptable from the results of the computer simulation based on the control-volume method. The thermal diffusivity was obtained from the difference of the temperature rate of change between heating and cooling modes, while, as described in a previous paper, the thermal conductivity was obtained from the temperature difference between the specimen surfaces and the specific heat capacity was derived from the thermal radiation power input into the specimen. Experimental results for Pyroceram 9606 and Pyrex 7740 specimens have confirmed the validity of the simultaneous measurements.

REFERENCES

1. S. B. Peralta, Z. H. Chen, and A. Mandelis, *Appl. Phys. A* **52**: 289 (1991).
2. K. Hisano, S. Sawai, and K. Morimoto, *Int. J. Thermophys.* **19**:316 (1998).
3. K. Hisano and F. Placido, *High Temp.-High Press.* **30**:287 (1998).
4. L. C. Hulstrom, R. P. Tye, and S. E. Smith, in *Proc. 19th Int. Conf. Therm. Conduct.* (Plenum, New York, 1987), p. 199.
5. K. Hisano, S Sawai, and K. Morimoto, *Int. J. Thermophys.* **19**:305 (1998).
6. R. Siegel and J. R. Howell, *Thermal Radiation Heat Transfer* (McGraw-Hill, New York 1972).
7. P. J. Roache, *Computational Fluid Dynamics* (Hermosa, Albuquerque, NM, 1976).
8. Y. S. Touloukian and E. H. Buyco, *Thermophysical Properties of Matter 5, Nonmetallic Solids, Specific Heat* (Plenum, New York, 1972).
9. T. S. Touloukian, *Thermophysical Properties of Matter 2. Nonmetallic Solids, Thermal Conductivity* (Plenum, New York, 1972).
10. M. M. Suliyanti, T. Baba, and A. Ono, in *Proc. 13th Japan Symp. Thermophys. Prop., Vol. 13* (Akita, 1992), p. 125.